2 μm mode-locking laser performances of sol-gel-fabricated large-core Tm-doped silica fiber

Yan Ren (任 艳)¹, Zhipeng Qin (覃治鹏)¹, Guoqiang Xie (谢国强)¹,*, Zhen Qiao (乔 桢)¹,
Ting Hai (海 婷)¹, Peng Yuan (袁 鹏)¹, Jingui Ma (马金贵)¹, Liejia Qian (钱列加)¹,
Shikai Wang (王世凯)², Chunlei Yu (于春雷)², and Lili Hu (胡丽丽)²

¹*Key Laboratory for Laser Plasmas of the Ministry of Education, Collaborative Innovation Center of IFSA (CICIFSA),*
School of Physics and Astronomy, Shanghai Jiao Tong University, Shanghai 200240, China
²*Key Laboratory of Materials for High Power Laser, Shanghai Institute of Optics and Fine Mechanics, Chinese Academy*
of Sciences, Shanghai 201800, China
*Corresponding author: xiegq@sjtu.edu.cn
Received September 10, 2017; accepted November 23, 2017; posted online January 31, 2018

High-power ultrafast fiber lasers operating at the 2 μm wavelength are extremely desirable for material processing, laser surgery, and nonlinear optics. Here we fabricated large-core (LC) double-cladding Tm-doped silica fiber via the sol-gel method. The sol-gel-fabricated Tm-doped silica (SGTS) fiber had a large core diameter of 30 μm with a high refractive index homogeneity ($\Delta n = 2 \times 10^{-4}$). With the newly developed LC SGTS fiber as the gain fiber, high-power mode-locking was realized. By using a semiconductor saturable absorber mirror (SESAM) as a mode locker, the LC SGTS fiber oscillator generated mode-locked pulses with an average output power as high as 1.0 W and a pulse duration of 23.9 ps at the wavelength of 1955.0 nm. Our research results show that the self-developed LC Tm-doped silica fiber via the sol-gel method is a promising gain fiber for generating high-power ultrafast lasers in the 2 μm spectral region.

OCIS codes: 060.2290, 060.3510, 140.4050, 140.3510.
doi: 10.3788/COL201816.020020.

Ultrafast lasers operating at the 2 μm wavelength have attracted wide interest due to their application potentiality in remote sensing, free-space optical communication, and pumping sources for mid-infrared super-continuum generation[1–3].

A Tm-doped silica fiber laser is an ideal way to generate high-power ultrashort pulses at the 2 μm wavelength. On the one hand, it has intrinsic advantages for high-power operation, including efficient heat dissipation, compactness, good beam quality, and high doping capability[4]. On the other hand, it simultaneously possesses the inherent merits of general Tm-doped gain media: it can be directly pumped by commercial 790 nm laser diodes (LDs); the quantum efficiency can be beyond 100% due to the existence of cross relaxation (CR) while pumping by 790-nm LDs. Furthermore, the wide emission spectrum of Tm-doped fiber allows the generation and amplification of ultrashort pulses near the 2 μm wavelength[5].

In general, generation of high-power ultrashort pulses is limited by the laser power density in the gain fiber. For mode-locking operation, high laser power density may lead to multiple pulsing, pulse collapse, harmonic mode-locking and noise-like mode-locking[6–9], etc., which significantly decrease the pulse peak power. To avoid the above effects and achieve high peak power, large-core (LC) silica fibers are developed. However, it is a challenge to fabricate rare-earth-doped LC silica fiber with the traditional methods such as axial vapor deposition (AVD), outside vapor-phase deposition (OVD) and the modified chemical vapor deposition method (MCVD). The AVD and OVD

methods can be used to fabricate LC silica fibers, but they cannot maintain good refractive index homogeneity in fibers, which is critical for realizing high laser beam quality[10]. The MCVD technology combined with solution doping has the merits of high purity and ultralow optical loss, and thus it has been the current standard industrial production method of fiber preforms[11]. However, it can only be used to fabricate silica fibers with a small core diameter[12]. In recent years, much effort has been made to develop an MCVD process combined with gas doping to prepare Yb-doped LC silica fibers[13–15], while it is currently still at the research stage. Recently, researchers at Jena University and the Heraeus company have developed a new powder sintering technology[16,17]. This non-CVD technology can prepare a Yb-doped silica rod with a high doping homogeneity. However, there is no report yet on Tm-doped silica fiber fabricated by this method. The sol-gel method combined with high-temperature sintering has great flexibility in preparing the geometry of silica glass, and different species of chemicals can be mixed in a molecular scale through the sol-gel method. Therefore, rare-earth-doped LC fiber with a high homogeneity can be realized via the sol-gel method[18,19].

In this work, we developed a type of LC double-cladding Tm-doped silica fiber via the sol-gel method. The self-developed sol-gel-fabricated Tm-doped silica (SGTS) fiber has a large core diameter of 30 μm with a high refractive index homogeneity ($\Delta n = 2 \times 10^{-4}$) that can support high-power mode-locked pulse generation. The continuous-wave (CW) laser test with 4 m

length SGTS fiber shows a slope efficiency of 18.85% with an output power of 1.6 W, and the output beam has a quasi-single mode characteristic ($M^2 = 1.3$). By using a semiconductor saturable absorber mirror (SESAM) as mode locker, the fiber laser with 4 m length SGTS fiber emits high-power mode-locked pulses with an average output power as high as 1.0 W, pulse energy of 43.1 nJ, and a pulse duration of 23.9 ps at 1955 nm wavelength. All the experimental results show that the LC double-cladding Tm-doped silica fiber fabricated via the sol-gel method is a promising gain fiber for generating ultrafast laser with high power and high beam quality.

In the fabrication process of SGTS fiber, tetraethoxysilane (TEOS), $AlCl_3 \cdot H_2O$, and $TmCl_3 \cdot 6H_2O$ were used as precursors. According to the required glass composition ($0.1Tm_2O_3$-$1.5Al_2O_3$-$98.4SiO_2$ in mol%), the mole ratio of $TmCl_3 \cdot 6H_2O$:$AlCl_3 \cdot 6H_2O$:TEOS was set to be 0.2: 3: 98.4. Hydrochloric acid and deionized water were added to sustain the hydrolysis reaction and then mixed for 24 h at 30°C with thorough stirring to form homogeneous and clear-doped sol. The sol was heated from 70°C to 1100°C to achieve dried gel powders with nearly complete decomposition of the organic components. Then the powder was sintered at 1750°C for 3 h in a vacuum to form Tm-doped bulk silica glass. A glass rod with a size of $\phi 3.2 \times 50$ mm was prepared as the preform core. The preform and an octagonal shaped pure silica glass as the inner cladding were prepared by the rod in tube method. The double cladding Tm-doped silica fiber with a core diameter of 30 μm and an outer cladding of an ultraviolet curing adhesive was prepared from the fiber drawing tower at a drawing temperature of 2020°C.

A 2 mm thickness polished glass slice cut from the original glass blank was used to study the spectroscopic properties of the SGTS core glass. Figures 1(a) and 1(b) show the
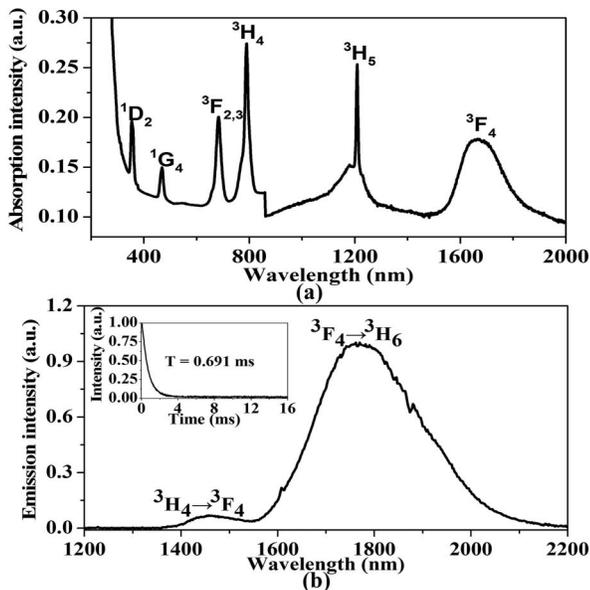
optical absorption spectrum and emission spectrum of the Tm-doped silica glass, respectively. Six absorption peaks corresponding to the transitions from the ground state $^3H_6$ to the excited states $^1D_2$, $^1G_4$, $^3F_2$, $^3H_4$, $^3H_5$, and $^3F_4$ are shown in Fig. 1(a). The two transitions $^3H_6 \rightarrow ^3H_4$ and $^3H_6 \rightarrow ^3F_4$ can be pumped by commercial 793 nm and 1570 nm LDs. The emission peak of the Tm fiber is at 1812 nm with a full width at half-maximum (FWHM) of 251.4 nm. Compared to the emission peak near 1812 nm, the emission of the $^3H_4 \rightarrow ^3F_4$ transition at 1.46 μm can be neglected[20]. According to the Fuchbauer-Ladenburg equations, the calculated peak emission cross section (σ_{emi}) is 6.86×10^{-21} cm^2 at 1812 nm. The measured fluorescence lifetime (τ) is 0.691 ms. The product of the peak emission cross section and the fluorescence lifetime is 4.74×10^{-21} cm$^2 \cdot$ ms[21], which is higher than that of the Tm-doped silica glass prepared by MCVD[22,23]. The large value of $\sigma_{emi} \times \tau$ is favorable for achieving a high laser gain.

In order to assess the homogeneity of the self-developed LC SGTS fiber, the radial refractive index profile of Tm-doped core glass and pure silica glass cladding was measured and the results are shown in Fig. 2. The measured refractive index fluctuation is as low as 2×10^{-4} in the core region, indicating that a high homogeneity is achieved via the sol-gel method combined with high-temperature sintering. The test error in Fig. 2 is an accumulated error caused by the PK2600 setup.

The CW and mode-locked laser performances of SGTS fiber were both tested in this Letter. The laser experimental setup schematic is depicted in Fig. 3. The 793 nm fiber-coupled LD was adopted as the pump source and the fiber had a core diameter of 105 μm and a

Fig. 1. Spectroscopic characteristics of LC SGTS fiber. (a) The absorption spectrum. (b) The fluorescence spectrum and fluorescence decay curve (inset) of the $^3F_4 \rightarrow ^3H_6$ transition.
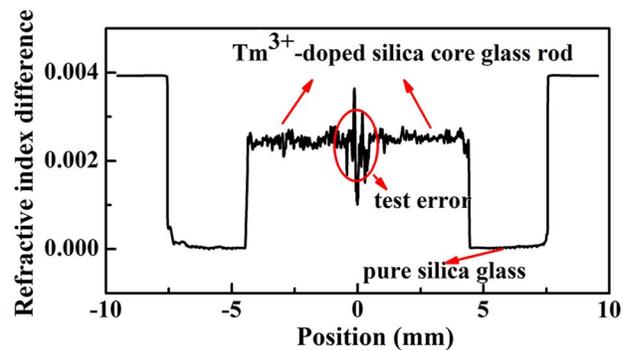
Fig. 2. Refractive index profile of the Tm-doped silica glass preform.
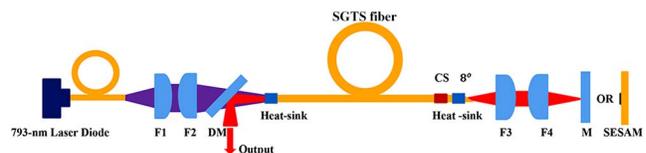
Fig. 3. Setup schematic of the laser experiments. DM: dichroic mirror; SGTS fiber: sol-gel fabricated Tm-doped silica fiber; CS: cladding stripper.

numerical aperture (NA) of 0.15. The pump light was collimated by a plano-convex lens F1 ($f_1 = 76$ mm), and then focused onto the gain fiber end by a plano-convex lens F2 ($f_2 = 75$ mm). The core diameter and NA value were 30 μm and 0.102, respectively, and the diameter and NA of the first cladding were 250 μm and 0.366, respectively. The gain fiber at the pump end was perpendicular-cleaved with a Fresnel reflection of 4% as cavity feedback and a transmission of 96% as output coupler. The other fiber end was cut with an angle of 8° to avoid parasitic oscillation. The SGTS fibers were coiled with a bending diameter of ∼20 cm. Both ends of the gain fiber were mounted in an aluminum heat sink with a V-groove to ensure efficient heat dissipation. The outer cladding of the fiber tail end near the SESAM was removed and coated with a cladding stripper to filter the pump light and prevent the SESAM from damage by
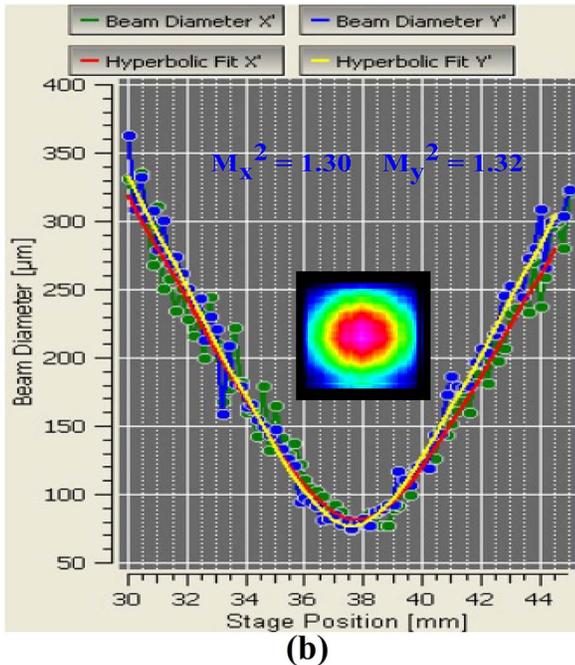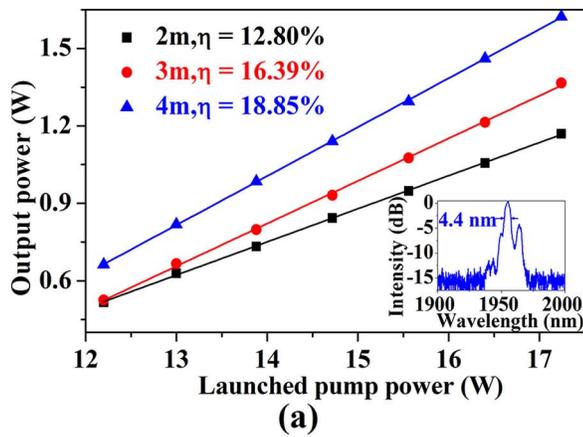
pump light. The laser from the fiber tail end was collimated and then focused onto the SESAM (or reflective mirror in CW operation) by a pair of plano-convex lenses F3 and F4 with the same focal length of 20 mm. The used commercial SESAM (BATOP GmbH SAM-1960-54-10ps) was designed to work at the wavelength of 1960 nm, and it had a modulation depth of 30%, a relaxation time of 10 ps, and a damage threshold of 800 μJ/cm². The 45°-placed dichroic mirror (DM), coated with high transmission for pump wavelength ($T > 95\%$) and high reflectivity for laser wavelength ($R > 99\%$), was used to separate the output laser beam from the pump light.

The CW laser performances with 2, 3, and 4 m SGTS fiber were first tested, and the results are shown in Fig. 4(a). As the launched pump power increased, the CW output power linearly increased with slope efficiencies of 12.80%, 16.39%, and 18.85% for 2, 3, and 4 m fiber, respectively. The slope efficiencies were smaller than those of fiber lasers with mature commercial Tm-doped silica fiber[24], which could be attributed to a larger optical loss in the present SGTS fiber[19]. The results show that the 4 m length LC double-cladding SGTS fiber has the best laser performance among them, which is attributed to a larger absorption of the pump light for the longer fiber. The maximum CW output power of 1.62 W was obtained, which was only limited by the available pump power in the experiment. There was no gain saturation at the highest CW output power, indicating that higher output power could be achieved providing a higher pump power. In this experiment, a mid-infrared spectrum analyzer with a resolution of 0.2 nm (Ocean Optics, SIR 5000) was adopted to measure the optical spectrum. The CW laser spectrum is shown in the inset of Fig. 4(a),

Fig. 4. (a) CW output power versus launched pump power. The inset shows the CW laser spectrum. (b) The M^2 factors of the output laser beam. Inset: output laser beam profile.
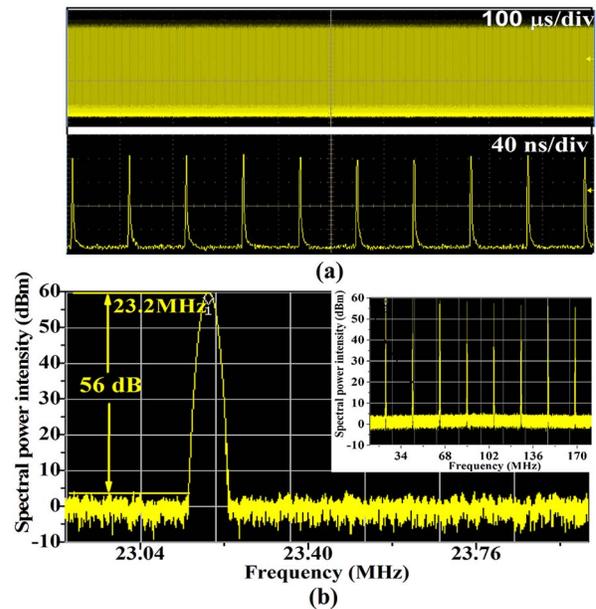
Fig. 5. (a) Mode-locked pulse trains in ms and ns time scales. (b) The radio frequency (RF) spectrum. Inset: the RF spectrum with a wide span.

which has a bandwidth of 4.4 nm centered at 1955 nm. The output beam quality was measured by a commercial beam profiler (Thorlabs, M2MS, 400–2700 nm). The measurement results are shown in Fig. 4(b). The beam quality factors in the X and Y directions were $M_x^2 = 1.30$ and $M_y^2 = 1.32$, respectively, suggesting that the laser operated in a quasi-single mode.

Then, we investigated the mode-locked laser performance with the 4 m length LC SGTS fiber as gain fiber. The setup of the mode-locked laser is shown in Fig. 3, in which the reflective mirror M is replaced by an SESAM. In the experiment, by accurately adjusting the SESAM to the focal plane of lens F4 (Fig. 3), stable CW mode-locking operation was achieved. When the launched pump power increased to 16.4 W, an average output power of 1.0 W was obtained.
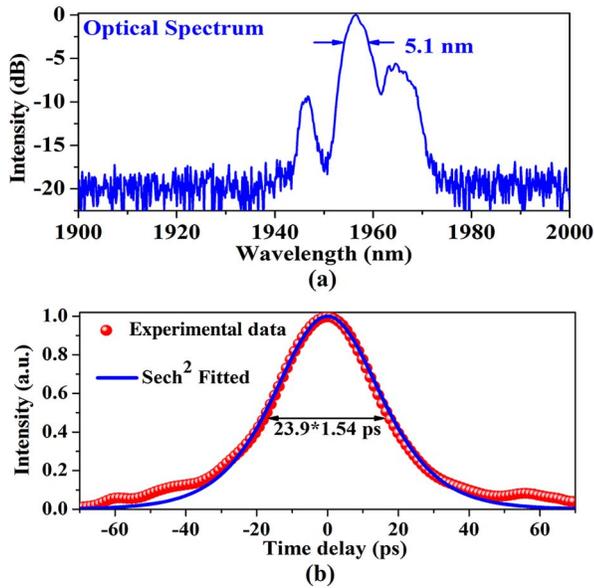
Fig. 6. (a) Optical spectrum. (b) The autocorrelation trace.

The typical performances of mode-locked pulses were measured at the average output power of 1.0 W. The mode-locked pulse trains in ms and ns time scales [Fig. 5(a)] indicate a stable CW mode-locking operation. The radio frequency (RF) spectrum (recorded by E4402B, Agilent) with a resolution bandwidth (RBW) of 20.0 kHz [Fig. 5(b)] shows a high signal-to-noise ratio of 56 dB, further indicating that the mode-locking was clean and stable. The mode-locked pulses had a repetition rate of 23.2 MHz. No multiple pulsing was observed at 1.0 W average output power, which benefits from the large core of the SGTS fiber.

The optical spectrum of the mode-locked pulses in Fig. 6(a) shows a central wavelength of 1955 nm with an FWHM of 5.1 nm. The spectral shape with two weak sidebands should be attributed to slight multi-mode operation in the laser, as seen in multi-mode fiber mode-locked lasers[25,26]. The autocorrelation trace (measured by APE pulse Check USB MIR) of the mode-locked pulses is shown in Fig. 6(b). Assuming a sech^2 pulse shape, the mode-locked pulse duration is 23.9 ps. According to the above results, the pulse energy and the peak power are calculated to be 43.1 nJ and 1.80 kW, respectively. Compared with other passively mode-locked Tm-doped fiber lasers (Table 1), the laser with SGTS fiber has a high average power and pulse energy, which benefits from the larger core diameter of the SGTS fiber. In this experiment, higher pulse energy was limited by the SESAM damage. It was possible to further scale up the output power and pulse energy by employing an SESAM with a higher damage threshold. To the best of our knowledge, it is the first time that a high-power mode-locked laser was demonstrated with the sol-gel-fabricated LC Tm-doped silica fiber.

In conclusion, an LC double-cladding Tm-doped silica fiber with a high homogeneity was fabricated via the sol-gel method and high-power mode-locking operation

Table 1. Passively Mode-locked Tm-doped or Tm/Ho co-doped Fiber Lasers Around 2 µm Spectral Region[a]

Mode-locking technique	Wavelength (nm)	Pulse width (ps)	Average power (mW)	Rep rate (MHz)	Pulse energy (nJ)	Reference
NPE	1842–1978	–	0.3–1.0	2.6	–	[27]
NPE	1880–2030	130	19	67.5	0.28	[28]
CNT	1930	1.32	3.4	37	10.88	[29]
CNT	1885	0.75	25	45	0.5	[30]
Graphene	1876	0.6	1.5	41	2.49	[31]
Graphene	1968	0.26	110	100.25	1.0	[32]
Graphene	1879.4	4.7	456	10	45.49	[33]
SESAM	1950	1.5	10	13.2	0.76	[34]
SESAM	1938	7.9	50	535	0.1	[35]
SESAM	1955	23.9	1.0×10^3	23.2	43.1	This work

[a]NPE: nonlinear polarization evolution, CNT: carbon nanotube, SESAM: semiconductor saturable absorber mirror.

with the fiber was demonstrated. The self-developed SGTS fiber has a large core diameter of 30 μm with a high refractive index homogeneity ($\Delta n = 2 \times 10^{-4}$). The CW laser performance test of the 4 m LC SGTS fiber shows a laser slope efficiency of 18.85% with an output power of 1.62 W. By using an SESAM as mode locker, the mode-locked laser with the 4 m length LC double-cladding SGTS fiber emitted an average output power as high as 1.0 W with a pulse duration of 23.9 ps at 1955 nm wavelength. All the experimental results show that the self-developed LC double-cladding Tm-doped silica fiber via the sol-gel method is a promising gain fiber for generating high-power ultrashort pulses at 2 μm wavelength.

References

1. W. Zeller, L. Naehle, P. Fuchs, F. Gerschuetz, L. Hildebrandt, and J. Koeth, Sensors **10**, 2492 (2010).
2. T. Brabec and F. Krausz, Rev. Mod. Phys. **72**, 545 (2000).
3. C. W. Rudy, A. Marandi, K. L. Vodopyanov, and R. L. Byer, Opt. Lett. **38**, 2865 (2013).
4. G. Sobon, Photon. Res. **3**, A56 (2015).
5. W. L. Barnes and J. E. Townsend, Electron. Lett. **26**, 746 (1990).
6. C. Lecaplain, P. Grelu, J. M. Soto-Crespo, and N. Akhmediev, J. Opt. **15**, 064005 (2013).
7. D. Faccio, M. Clerici, A. Averchi, A. Lotti, O. Jedrkiewicz, A. Dubietis, G. Tamosauskas, A. Couairon, F. Bragheri, D. Papazoglou, S. Tzortzakis, and P. Di Trapani, Phys. Rev. A **78**, 033826 (2008).
8. H. Yu, X. Zheng, K. Yin, X. A. Cheng, and T. Jiang, Laser Phys. **27**, 015102 (2017).
9. S. Liu, F. P. Yan, L. N. Zhang, W. G. Han, Z. Y. Bai, and H. Zhou, J. Opt. **18**, 015508 (2016).
10. E. Potkay, H. R. Clark, I. P. Smyth, T. Y. Kometani, and D. L. Wood, J. Lightwave Technol. **6**, 1338 (1988).
11. S. Poole, D. Payne, R. Mears, M. Fermann, and R. Laming, J. Lightwave Technol. **4**, 870 (1986).
12. A. Langner, G. Schotz, M. Such, T. Kayser, V. Reichel, S. Grimm, J. Kirchhof, V. Krause, and G. Rehmann, Proc. SPIE **6873**, U157 (2008).
13. V. Petit, R. P. Tumminelli, J. D. Minelly, and V. Khitrov, Proc. SPIE **9728**, 97282R (2016).
14. T. F. Shi, Z. G. Zhou, L. Ni, X. S. Xiao, H. Zhan, A. D. Zhang, and A. X. Lin, Appl. Opt. **53**, 3191 (2014).
15. K. K. Bobkov, M. Y. Koptev, A. E. Levchenko, S. S. Aleshkina, S. L. Semenov, A. N. Denisov, M. M. Bubnov, D. S. Lipatov, A. Y. Laptev, A. N. Guryanov, E. A. Anashkina, S. V. Muravyev, A. V. Andrianov, A. V. Kim, and M. E. Likhachev, Proc. SPIE **10083**, 1008309 (2017).
16. M. Leich, F. Just, A. Langner, M. Such, G. Schotz, T. Eschrich, and S. Grimm, Opt. Lett. **36**, 1557 (2011).
17. W. B. He, M. Leich, S. Grimm, J. Kobelke, Y. Zhu, H. Bartelt, and M. Jager, Laser Phys. Lett. **12**, 015103 (2015).
18. A. Baz, H. El Hamzaoui, I. Fsaifes, G. Bouwmans, M. Bouazaoui, and L. Bigot, Laser Phys. Lett. **10**, 055106 (2013).
19. F. G. Lou, P. W. Kuan, L. Zhang, S. K. Wang, Q. L. Zhou, M. Wang, S. Y. Feng, K. F. Li, C. L. Yu, and L. L. Hu, Opt. Mater. Express **4**, 1267 (2014).
20. E. R. Taylor, L. N. Ng, N. P. Sessions, and H. Buerger, J. Appl. Phys. **92**, 112 (2002).
21. T. F. Xue, L. Y. Zhang, L. Wen, M. S. Liao, and L. L. Hu, Chin. Opt. Lett. **13**, 081602 (2015).
22. M. Engelbrecht, F. Haxsen, D. Wandt, and D. Kracht, Opt. Express **16**, 1610 (2008).
23. S. D. Agger and J. H. Povlsen, Opt. Express **14**, 50 (2006).
24. C. Kneis, B. Donelan, A. Berrou, I. Manek-Hönninger, T. Robin, B. Cadier, M. Eichhorn, and C. Kieleck, Opt. Lett. **40**, 1464 (2015).
25. L. G. Wright, D. N. Christodoulides, and F. W. Wise, "Spatiotemporal mode-locking in multimode fiber lasers," https://arxiv.org/abs/1705.05050 (2017).
26. Y. Wang, S. Yan, J. Xu, and Y. Tang, "Developing spatiotemporal solitons in step-index multimode fibers," https://arxiv.org/abs/1607.05388 (2016).
27. Z. Yan, B. Sun, X. Li, J. Luo, P. P. Shum, X. Yu, Y. Zhang, and Q. J. Wang, Sci. Rep. **6**, 27245 (2016).
28. Y. Nomura, M. Nishio, S. Kawato, and T. Fuji, IEEE J. Sel. Top. Quantum Electron. **21**, 24 (2015).
29. M. A. Solodyankin, E. D. Obraztsova, A. S. Lobach, A. I. Chernov, A. V. Tausenev, V. I. Konov, and E. M. Dianov, Opt. Lett. **33**, 1336 (2008).
30. K. Kieu and F. W. Wise, IEEE Photonics Technol. Lett. **21**, 128 (2009).
31. G. Sobon, J. Sotor, I. Pasternak, A. Krajewska, W. Strupinski, and K. M. Abramski, Opt. Express **23**, 9339 (2015).
32. G. Sobon, J. Sotor, I. Pasternak, A. Krajewska, W. Strupinski, and K. M. Abramski, Opt. Express **23**, 31446 (2015).
33. X. Li, X. Yu, Z. Sun, Z. Yan, B. Sun, Y. Cheng, X. Yu, Y. Zhang, and Q. J. Wang, Sci. Rep. **5**, 16624 (2015).
34. Q. Wang, J. Geng, T. Luo, and S. Jiang, Opt. Lett. **34**, 3616 (2009).
35. P. W. Kuan, K. Li, L. Zhang, X. Li, C. Yu, G. Feng, and L. Hu, IEEE Photonics Technol. Lett. **28**, 1525 (2016).